

# General Framework for phase synchronization through localized sets

T. Pereira, M.S. Baptista, and J. Kurths

*Nonlinear Dynamics, Institute of Physics,  
University of Potsdam, D-14415, Potsdam, Germany*

(Dated: October 26, 2018)

## Abstract

We present an approach which enables to identify phase synchronization in coupled chaotic oscillators without having to explicitly measure the phase. We show that if one defines a typical event in one oscillator and then observes another one whenever this event occurs, these observations give rise to a localized set. Our result provides a general and easy way to identify PS, which can also be used to oscillators that possess multiple time scales. We illustrate our approach in networks of chemically coupled neurons. We show that clusters of phase synchronous neurons may emerge before the onset of phase synchronization in the whole network, producing a suitable environment for information exchanging. Furthermore, we show the relation between the localized sets and the amount of information that coupled chaotic oscillator can exchange.

## I. INTRODUCTION

The emergency of collective behavior among coupled oscillators is a rather common phenomenon. In nature, one typically finds interacting chaotic oscillators which through the coupling scheme form small and large networks. Surprisingly, even though chaotic systems possess an exponential divergency of nearby trajectories, they can synchronize due to the coupling, still preserving the chaotic behavior[1, 2, 3]. Indeed, synchronization phenomena have been found in a variety of fields as ecology [4], neuroscience [5, 6, 7], economy [8], and lasers [9, 10, 11].

In the last years some types of synchronization have been reported [12]. A rather interesting kind is a weak synchronization, namely phase synchronization (PS), that does not reveal itself directly from the trajectory, but as a boundedness of phase difference between the interacting oscillators. In such a synchronization the trajectories can be uncorrelated, and therefore, the oscillators present some independence of the amplitudes, but still preserving the collective behavior.

This phenomenon can arise from a very small coupling strength [13]. It has been reported that it mediates processes of information transmission and collective behavior in neural and active networks [14], and communication processes in the human brain [15, 16]. Its presence has been found in a variety of experimental systems, such as in electronic circuits [17, 18], in electrochemical oscillators [19], plasma physics [20], and climatology [21].

In order to state the existence of PS, one has to introduce a phase  $\phi(t)$  for the chaotic oscillator, what is not straightforward. Even though the phase is expected to exist to a general attractor, due to the existence of the zero Lyapunov exponent [12], its explicit calculation may be impossible. Actually, even for the simple case of coherent attractors, it has been shown that phases can be defined in different ways, each one being chosen according to the particular case studied. However, all of them agree for sufficiently coherent attractors [22].

In spite of the large interest in this field, there is still no general, systematic, and easy way to detect the existence of this phenomenon, mainly, due to the fact that the phase is rather difficult (often unknown) to calculate. The calculation becomes even harder if the oscillators are non-coherent, e.g. the funnel oscillator [12]. Therefore, in order to present a general approach to detect PS, with practical applications, we must overcome the need of a

phase.

In many cases the phase can be estimated via the Hilbert transformation or a wavelet decomposition [12]. Supposing that it is possible to get a phase, the approach developed in Ref. [23] gives rather good results. It is grounded on the idea of conditional observations of the oscillators. Whenever the phase of one of the oscillators is increased by  $2\pi$ , we measure the phase of the other oscillators. The main idea is that if one has PS, the distribution of these conditional observation in the phase presents a sharp peak, and therefore PS can be detected.

There are a few approaches that try to overcome the difficulties of not having a general phase. For periodically driven oscillators, there is an interesting approach, very useful and easy to implement that overcomes the need of a phase, the stroboscopic map technique. It consists in sampling the chaotic trajectory at times  $nT_0$ , where  $n$  is an integer and  $T_0$  is the period of the driver. The stroboscopic map was used to detect PS [12, 18, 20]. The basic idea is that if the stroboscopic map is localized in the attractor, PS is present. Actually, the stroboscopic map is a particular case of the approach of Ref. [23]. Indeed, since the driver is periodic, the observation of the trajectory of the chaotic oscillators at times  $nT_0$  is equivalent to observe the oscillators at every increasing of  $2\pi$  in the phase of the driver. Furthermore, if the chaotic oscillator presents a sharp conditional distribution, this means that the stroboscopic map is localized. The advantage of such an approach is that it does not require the introduction of a phase neither in the periodic oscillator nor in the chaotic one.

In the case of two or more coupled chaotic oscillators, namely  $\Sigma_j$  and  $\Sigma_k$ , the stroboscopic map techniques can be no longer applied. However, if the oscillators are coherent and have a proper rotation, a generalization of the stroboscopic map has been recently developed [24]. Instead of observing the oscillators at fixed time intervals, multiples of the period, one can define a Poincaré section in  $\Sigma_j$  and then observe  $\Sigma_k$  every time the trajectory of  $\Sigma_j$  crosses the Poincaré section. If the oscillators are in PS, these observations give place to a localized set.

Another approach that is relevant to the present problem is the one developed in Ref. [25]. This approach consists of defining a point  $\mathbf{x}_j(t) \in \Sigma_j$  and a small neighborhood of this point composed by points  $\mathbf{x}_j(t_i) \in \Sigma_j$ , where  $i = 1, \dots, N$ , with  $N$  being the number of points within the defined neighborhood. Then, one observes the oscillator  $\Sigma_k$  at the times  $t_i$ ,

which gives place to the points  $\mathbf{x}_k(t_i) \in \Sigma_k$ . Again, the idea is that if the oscillators present synchronization, the cloud of points  $\mathbf{x}_k(t_i)$  occupies an area much smaller than the attractor area. Further, estimators have been introduced to quantify the amount of synchronization [25].

Even though the intuition says that localized set implies the presence of synchronization, there is a lack of theoretical analysis showing such a result for a general oscillator. Moreover, as far as we know, there are no results that guarantee that such an approach works for multiple time-scale oscillators. In addition, it is not clear what kind of points (events) could be chosen, and finally, how one should proceed in the case that the small neighborhood of the point  $\mathbf{x}_j(t) \in \Sigma_j$  has infinitely many neighbor points.

In this work, we extend the ideas of Ref. [12, 18, 20, 24, 25]. We show that all these approaches can be put in the framework of localized sets. Our results demonstrate that for general coupled oscillators  $\Sigma_j$  and  $\Sigma_k$ , if one defines a typical event in  $\Sigma_j$  and then observes the oscillator  $\Sigma_k$  whenever this event occurs, these observations give rise to a localized set in the accessible phase space if PS exists. These results can be applied to oscillators that possess multiple time-scales as well as in neural networks. As an application, we analyze the onset of PS in neural networks. We show that in general neural networks one should expect to find clusters of phase synchronized neurons that can be used to transmit information in a multiplexing and multichannel way. Finally, we relate the localized sets from our theory to the information exchange between the coupled chaotic oscillators.

The paper is organized as follows: In Sec. II we define the dynamical systems we are working on. In Sec. III we give a result that enables the identification of PS without having to measure the phase. We illustrate these findings with two coupled Rössler oscillators in Sec. IV. For oscillators possessing multiple time-scales our main results are discussed in Sec. V, and then illustrated in Sec. VI for bursting neurons coupled via inhibitory synapses. Our results are also applied to neural networks of excitatory neurons in Sec. VII. We briefly discuss how to apply these ideas into high dimension oscillators and experimental data series in Sec. VIII. Finally, we analyze the relation between the localized sets and the transmission of information in chaotic oscillators in Sec. IX. Moreover, in Appendix A we prove the main theorem of Sec. III about the localization of sets in PS.

## II. BASIC SET UP

We consider  $N$  oscillators given by first order coupled differential equations:

$$\dot{\mathbf{x}}_i = \mathbf{F}_i(\mathbf{x}_i) + \sum_{j=1}^N C_{ij} \mathbf{H}_j(\mathbf{x}_j, \mathbf{x}_i) \quad (1)$$

where,  $\mathbf{x}_i \in \mathbb{R}^{n_i}$ , and  $\mathbf{F}_i : \mathbb{R}^{n_i} \rightarrow \mathbb{R}^{n_i}$ ,  $\mathbf{H}_j$  is the output vector function, and  $C_{ij}$  is the coupling strength between  $j$  and  $i$ . Note that  $C_{ij}$  could also depend on the coordinates and on time. From now on, we shall label the coupled oscillator  $\mathbf{x}_i$  by subsystem  $\Sigma_i$ . Next, we assume that each  $\Sigma_j$  has a stable attractor, i.e. an inflowing region of the phase space where the solution of  $\Sigma_j$  lies. Further, we assume that the subsystem  $\Sigma_j$  admits a phase  $\phi_j(t)$ . Therefore, the condition for PS between the oscillators  $\Sigma_j$  and  $\Sigma_k$  can be written as:

$$|m\phi_j(t) - n\phi_k(t)| < c, \quad (2)$$

where  $n$  and  $m$  are integers, and the inequality must hold for all times, with  $c$  being a finite number. For a sake of simplicity, we consider the case where  $n = m = 1$ , in other words  $1 : 1$  PS. Herein, we suppose that a frequency  $\Omega_j$  can be defined in each subsystem  $\Sigma_j$ , such that:

$$\dot{\phi}_j = \Omega_j(\mathbf{x}_1, \dots, \mathbf{x}_N, t), \quad (3)$$

where  $\Omega_j$  is a continuous function bounded away from zero. Furthermore there is a number  $M$  such that  $\Omega_j \leq M$ . This phase is an abstract phase in the sense that it is well defined, but we are not able to write the function  $\Omega_j$  for a general oscillator. We also consider the frequencies  $\dot{\phi}_j$  not to be too different, such that, in general, through the coupling PS can be achieved.

## III. LOCALIZED SETS IN PS STATES

In this section we present our main result. The basic idea consists in the following: Given two subsystems  $\Sigma_k$  and  $\Sigma_j$ , we observe  $\Sigma_k$  whenever an event in the oscillator  $\Sigma_j$  happens. As a consequence of these conditional observations, we get a set  $\mathcal{D}_k$ . Depending on the properties of this set one can state whether there is PS.

The conditional observations could be given by a Poincaré section, if it is possible to define a Poincaré Section with the property that the trajectory crosses it once per cycle in a

given direction. We wish to point out that in this case, one is able to have more information about the dynamics and the phase synchronization phenomenon. As an example, one can introduce a phase, and estimate the average frequency of the oscillators. However, these techniques based on the Poincaré section [12, 24] cannot be applied to attractors without a proper rotation, where such a section cannot be well defined.

Our main result overcomes the need of a Poincaré Section. We show that one can use any typical event to detect PS. Such events may be the crossing of the trajectory with a small piece of a Poincaré section (when it is possible to defined such a section), the crossing of the trajectory with an arbitrary small segment, the entrance of the trajectory in an  $\varepsilon$ -ball, and so on. The only constraint is that the event must be typical (we shall clarify what we mean by typical, later on ) and the region where the event is defined must have a positive measure. Let  $(t_{k,j}^i)_{i \in \mathbb{N}}$  be the time at which the  $i$ th event in the subsystem  $\Sigma_{k,j}$  happens. Then, we construct the set:

$$\mathcal{D}_k \equiv \cup_{i \in \mathbb{N}} \mathbf{F}^{t_j^i}(\mathbf{x}_k^0), \quad (4)$$

where  $\mathbf{x}_k^0$  is the initial point within the attractor of  $\Sigma_k$ . Next, we define what we understand by localized set.

**Definition 1** *Let  $\mathcal{D}_j$  be a subset of  $\Phi_j$ . The set  $\mathcal{D}_j$  is localized in  $\Phi_j$  if there is a cross section  $\Psi_j$  and a neighborhood  $\Lambda_j$  of  $\Psi_j$  such that  $\mathcal{D}_j \cup \Lambda_j = \emptyset$*

An illustration of the definition is given in Fig. 1.

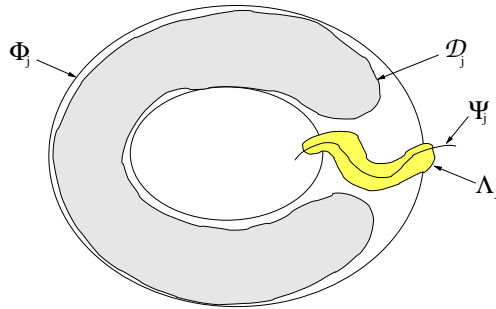


FIG. 1: (Color online) An illustration of the Def. 1. The set  $\mathcal{D}_j$  does not intersect the neighborhood  $\Lambda_j$ , therefore,  $\mathcal{D}_j$  is a localized set of  $\Phi_j$ .

Under the assumptions of Sec. II, the following result connects the existence of phase synchronization with the localization of sets the  $\mathcal{D}$ :

**Theorem 1** *Given a typical event, with positive measure, in the oscillator  $\Sigma_j$ , generating the times  $(t_j^i)_{i \in \mathbb{N}}$ . The observation of  $\Sigma_k$  at  $(t_j^i)_{i \in \mathbb{N}}$  generates a localized set  $\mathcal{D}_k$  if there is PS.*

This result constitutes a direct generalization of approaches of Refs. [24, 25]. As a consequence, this result shed a light into the problem of PS detection, which turned out to be a rather difficult task, depending on the system faced. Therefore, PS can be detected in real-time experiments and in data analysis by verifying whether the sets  $\mathcal{D}$  are localized, without needing any further calculations.

#### A. Connection between $\mathcal{D}$ and Unstable Periodic Orbits

In this section we investigate the mechanism for the non localization of the sets  $\mathcal{D}$ . We let the event definition be an entrance in an  $\varepsilon$ -ball in both subsystems, with  $\varepsilon$  being the radius. When  $\varepsilon$  is small enough, we can demonstrate that PS leads to the locking of all unstable periodic orbits (UPO) between the subsystems.

**Proposition 1** *If the set  $\mathcal{D}_k$  is localized, then all UPOs between  $\Sigma_k$  and  $\Sigma_j$  are locked.*

**Proof:** We demonstrate this result by absurd. Let us assume that there is PS; as a consequence the set  $\mathcal{D}_k$  is localized. Suppose that there is an UPO, regarded as  $\mathcal{X}_j$  in  $\Sigma_j$ , and another UPO, regarded as  $\mathcal{X}_k$  in  $\Sigma_k$ , and that they are not locked (there is no rational number that relates both frequencies). So, there is a mismatch between the frequencies of the two UPOs. Given an  $\varepsilon_j$ -ball around  $\mathbf{y}_j^0$  (resp.  $\mathbf{y}_k^0$ ), where  $\mathbf{y}_j^0 \in \mathcal{X}_j$  (resp.  $\mathbf{y}_k^0 \in \mathcal{X}_k$ ), any point  $\mathbf{x}_j$  distant  $\delta_j$  from  $\mathbf{y}_j^0$ , where  $\delta_j \ll \varepsilon_j$ , follows  $d[\mathbf{F}_j^t(\mathbf{x}_j), \mathbf{F}_j^t(\mathbf{y}_j^0)] \leq \varepsilon_j$ , for any  $t \leq \tilde{t} \approx \ln(\varepsilon_j/\delta_j)/\lambda_{max}$ , where  $\lambda_{max}$  is the largest eigenvalue associated with the orbit  $\mathcal{X}_j$ , and  $d[\cdot, \cdot]$  is a metric. An initial condition inside the  $\delta_j$ -ball is governed by the UPO  $\mathcal{X}_j$  till a time  $t \leq \tilde{t}$ , see Fig. 2 for an illustration. Next, we construct the set  $\mathcal{D}_k$  by sampling the trajectory of  $\Sigma_k$  whenever the trajectory  $\Sigma_j$  enters in the  $\varepsilon$ -ball, which is equivalent to observe  $\Sigma_k$  every period of the UPO  $\mathcal{X}_j$ . There is an one-to-one correspondence (isomorphism) between the dynamics of the conditional observations and the dynamics of the irrational rotation in the unitary circle,  $R_\alpha : S^1 \rightarrow S^1$ ,  $R_\alpha = e^{i\alpha\sqrt{-1}}z$ , where  $\alpha$  is the frequency mismatch between the two UPOs, here given by:

$$\alpha = \inf_{a,b} \{a \times \omega_{\mathcal{X}_j} - b \times \omega_{\mathcal{X}_k}\}, \quad (5)$$

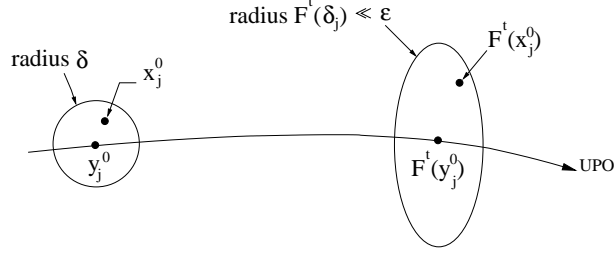


FIG. 2: Illustration of the dynamics near a UPO.

where  $\omega_{\mathcal{X}_{j,k}}$  is the angular frequency of  $\mathcal{X}_{j,k}$ . This means that the points of  $\mathcal{D}_k$  will be dense around the UPO  $\mathcal{X}_k$ , and therefore, the set  $\mathcal{D}_k$  is not localized; there is no PS, what contradict our assumption. Indeed, since  $\Delta\omega \geq 0$ , it is impossible to bound the phase difference between  $\Sigma_j$  and  $\Sigma_k$  by a finite number. Thus, in order to have localized sets  $\mathcal{D}$ , all UPOs must be locked.  $\square$

This shows that the mechanism for the non-localization of the sets  $\mathcal{D}$  will be the existence of unlocked UPOs between  $\Sigma_j$  and  $\Sigma_k$ . Similar results have been pursued for periodically driven oscillators, [12]. Right at the desynchronization some UPOs become unlocked and the stroboscopic map becomes non-localized, and some phase slips happen, generating an intermittent behavior. The duration of the phase slips are related to the number of unlocked UPOs. Of course, in this regime the set  $\mathcal{D}$  is a non-localized set. However, if one looks for finite time intervals the set  $\mathcal{D}$  may be apparently localized.

#### IV. COUPLED RÖSSLER OSCILLATORS

We first illustrate this result for two coupled Rössler oscillators, given by:

$$\begin{aligned} \dot{x}_{1,2} &= -\alpha_{1,2}y_{1,2} - z_{1,2} + \epsilon(x_{2,1} - x_{1,2}), \\ \dot{y}_{1,2} &= \alpha_{1,2}x_{1,2} + 0.15y_{1,2}, \\ \dot{z}_{1,2} &= 0.2 + z_{1,2}(x_{1,2} - 10), \end{aligned} \tag{6}$$

with  $\alpha_1 = 1$ , and  $\alpha_2 = \alpha_1 + \delta\alpha_2$ . In such a coherent oscillator, we can simply define a phase  $\tan\phi_i = y_i/x_i$ , where  $i = 1, 2$ , which provides an explicit equation for it. Indeed, taking the derivative with respect to time:

$$\frac{\partial}{\partial\phi_i}\tan(\phi_i) \times \dot{\phi}_i = \frac{d}{dt}\frac{y_i}{x_i}, \tag{7}$$



which can be written as  $\sec^2(\phi_i) \times \dot{\phi}_i = (\dot{y}_i x_i - y_i \dot{x}_i)/x_i^2$ , which provides:

$$\phi_i(t) = \int_0^t \frac{\dot{y}_i x_i - \dot{x}_i y_i}{x_i^2 + y_i^2} dt, \quad (8)$$

noting that  $\sec^2 \phi_i = (x_i^2 + y_i^2)/x_i^2$ . In a more compact notation, we consider  $\mathbf{x}_i = (x_i, y_i)$ , then Eq. (8) can be written as

$$\phi_i(t) = \int_0^t \frac{\dot{\mathbf{x}}_i \wedge \mathbf{x}_i}{|\mathbf{x}_i|^2} dt, \quad (9)$$

where  $\wedge$  represents the vectorial product. Equation (9) can be used to calculate the phase of the oscillators  $\Sigma_i$ , and there is PS if  $\Delta\phi = \phi_2 - \phi_1$  remains bounded as  $t \rightarrow \infty$ .

In order to apply our results we may define an event occurrence in both oscillators. We define the event in oscillator  $\Sigma_1$  to be the trajectory crossing with the segment:

$$\mathcal{S}_1 = \{x_1, y_1, z_1 \in \mathbb{R} | x_1 < -13, y_1 = 0, \text{ and } \dot{y}_1 > 0\}, \quad (10)$$

the crossings generate the times  $(t_1^i)_{i \in \mathbb{N}}$ . The event in the oscillator  $\Sigma_2$  happens whenever its trajectory crosses the segment:

$$\mathcal{S}_2 = \{x_2, y_2, z_2 \in \mathbb{R} | x_2 > 5, y_2 = 10, \text{ and } \dot{y}_2 < 0\}, \quad (11)$$

the crossings generates the times  $(t_2^i)_{i \in \mathbb{N}}$ . Then, the set  $\mathcal{D}_{2,1}$  is constructed by observing the oscillators  $\Sigma_{2,1}$  at times  $(t_{1,2}^i)_{i \in \mathbb{N}}$

For  $\epsilon = 0.001$  and  $\Delta\alpha_2 = 0.001$ , the set  $\mathcal{D}_1$  spreads over the attractor of  $\Sigma_1$  [ Fig 3 (a)], and  $\mathcal{D}_2$  spreads over the attractor of  $\Sigma_2$  [ Fig. 3(b)]. Therefore, there is no PS, i.e. the phase difference  $\Delta\phi$  diverges [Fig 3 (e)]. Indeed, a calculation of the frequencies shows that  $\langle \dot{\phi}_1 \rangle = 1.03479$  and  $\langle \dot{\phi}_2 \rangle = 1.03508$ . As we increase the coupling, PS appears. In particular, for  $\epsilon = 0.011$  and  $\Delta\alpha = 0.001$ , the sets  $\mathcal{D}_1$  and  $\mathcal{D}_2$  are localized [Figs 3 (c) and (d), respectively]. Hence, the phase difference is bounded [Fig. 3(f)]. The average frequency is  $\langle \dot{\phi}_1 \rangle = \langle \dot{\phi}_2 \rangle = 1.03522$ .

### A. Estimating the synchronization level

Our main goal is to state the existence of PS, however, we can also estimate the synchronization level between  $\Sigma_j$  and  $\Sigma_k$  by means of the localized sets. This can be done by introducing an estimator  $H_{jk}$ . One way to estimate the amount of synchrony is to define:

$$H_{jk} = \frac{\text{vol of } \mathcal{D}_j}{\text{vol of the attractor of } \Sigma_j}, \quad (12)$$

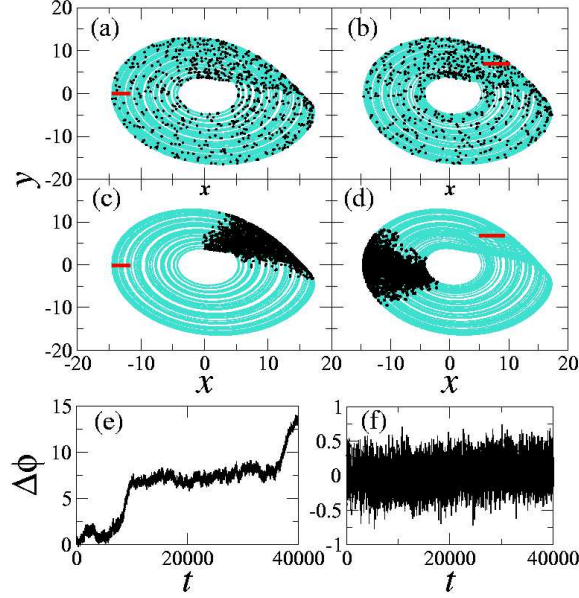


FIG. 3: (Color online) PS onset in two coupled Rössler oscillators. In (a,c) we depict the attractor of the oscillator  $\Sigma_1$  and in (b,d) the attractor of  $\Sigma_2$  in light gray, the sets  $\mathcal{D}$  are depicted in black. The bars on Figs. (a) and (c) represent the segment  $\mathcal{S}_1$ , while in Figs. (b) and (d) the segment  $\mathcal{S}_2$ . In (a) and (b) the sets  $\mathcal{D}_1$  and  $\mathcal{D}_2$  spread over the attractor of the oscillator  $\Sigma_1$  and  $\Sigma_2$ , respectively; and there is no PS, the phase difference diverges (e). The parameters are  $\epsilon = 0.001$  and  $\Delta\alpha = 0.001$ . In (c) and (d) the sets  $\mathcal{D}_1$  and  $\mathcal{D}_2$ , respectively, are localized and there is PS; the phase difference is bounded (f). The parameters are  $\epsilon = 0.011$  and  $\Delta\alpha = 0.001$ .

where  $\text{vol}$  denotes the volume [26]. If there is no PS, the set  $\mathcal{D}_j$  spreads over the attractor of  $\Sigma_j$ , see Fig. 3(a,b), then,  $H_{ij} = 1$ . As the oscillators undergo a transition to PS,  $H_{jk}$  becomes smaller than 1. The lower  $H_{jk}$  is the stronger the synchronization level is [27].

For attractors with the same topology as the Rössler oscillator,  $H_{jk}$  can be easily calculated. Instead of computing the volume, we calculate the area occupied by the attractor in the plane  $(x, y)$ . The area  $A_j$  of the attractor of  $\Sigma_j$  can be roughly estimated by the area of the disk with radii  $r_m$  and  $r_M$ , see Fig. 4. Thus,  $A_j = \pi(r_M^2 - r_m^2)$ . On the other hand, the set  $\Sigma_j$  is confined into an angle  $\xi$  [Fig. 4]. Therefore, the area of the set  $\mathcal{D}_j$  can be estimated as  $\xi(r_M^2 - r_m^2)/2$ . Thus, the estimator can be written as:

$$H_{jk} = \frac{\xi}{2\pi} \quad (13)$$

We have used Eq. (13) to estimate the amount of synchronization between the two

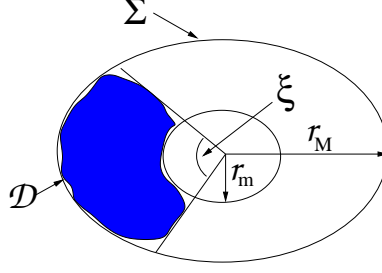


FIG. 4: (Color online) Illustration of a localized set in a Rössler like attractor. The attractor can be approximated by a disk with major radius  $r_M$  and minor radius  $r_m$ . The sets  $\mathcal{D}$  are confined within an angle  $\xi$ .

coupled Rössler of Eq. (6). We fix  $\epsilon = 0.001$  and vary the mismatch parameter  $\delta\alpha$  within the interval  $[-0.002, 0.002]$ . For  $|\delta\alpha| \approx 0.0009$  the coupled Rösslers phase synchronize, which means that the set  $\mathcal{D}_j$  is localized. Therefore,  $H_{jk} < 1$ . The smaller the value of  $|\delta\alpha|$  is the more localized the set  $\mathcal{D}_j$  becomes, meaning that the oscillators are more synchronized, leading  $H_{jk}$  to low values. At  $|\delta\alpha| = 0$  the two coupled oscillators present their strongest synchronization with  $H_{jk} \approx 0.22$ . The results are depicted in Fig. 5.

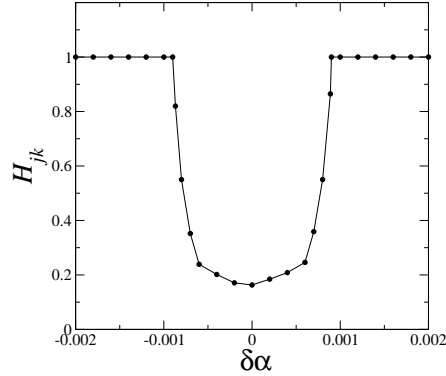


FIG. 5:  $H_{jk}$  is depicted for the two coupled Rösslers, Eq. (6), with  $\epsilon = 0.001$ . The estimator  $H_{jk}$  is computed by means of Eq. (13), whenever  $H_{ij} = 1$  there is no PS. At  $|\delta\alpha| \approx 0.0009$  the coupled Rösslers undergo a transition to PS, and therefore,  $H_{jk} < 1$ , which shows the presence of PS.

## V. OSCILLATORS WITH MULTIPLE TIME-SCALES

In oscillators with only one time-scale, i.e. one typical period, a typical event means an event possible to realize, thus with positive measure. In oscillators with multiple time-scales, i.e. oscillators that possess more than one typical period (an oscillator with a fast and slow variables), a typical event means an event that takes into account all time-scales. Conversely, an atypical event is the one that takes into account just a few time-scales, e.g. only one. In such an oscillator with multiple time-scales, one may have synchronization only in one time scale, while the others may be asynchronous. If the event definition excludes completely the dynamics of the synchronized time-scale this event is atypical and one does not observe localized sets through it. In order to clarify these ideas, we consider two instructive examples.

### A. Dynamics on a Torus

Let us consider a quasi-periodic motion on a torus  $T^2$  with two independent frequencies  $\omega$  and  $\alpha$ , i.e.  $n\omega - m\alpha \neq 0 \ \forall n, m \in \mathbb{Z}$ . The dynamics on the torus  $\Sigma_k : T^2 \rightarrow T^2$  can be characterized by the angular variables and the flow takes the form  $\Omega_k = (u, v) = (\omega t + \omega_0, \alpha t + \alpha_0)$ . Furthermore, we consider another oscillator on a quasi-periodic torus with two independent frequencies  $\omega$  and  $\beta$ , the flow  $\Sigma_j : T^2 \rightarrow T^2$ , in angular variables, takes the form  $\Omega_j = (g, h) = (\omega t + \tilde{\omega}_0, \beta t + \beta_0)$ . Therefore, under this construction one sees PS in only one time-scale, since  $\alpha, \beta$  are independent.

If we consider the event in the oscillator  $\Sigma_k$  to be the increasing of  $2\pi$  on the variable  $u$ , conversely the crossing in the section  $\mu$ , it generates the times  $t_k^i = 2\pi \times i/\omega$ . The observation of  $\Sigma_j$  at these times generates a localized set  $\mathcal{D}_j$ , which will lay on  $S^1$ , a subset of  $T^2 = S^1 \times S^1$ , and will never occupy the full space. On the other hand, if we consider the event in the oscillator  $\Sigma_j$  to be the increasing of  $\pi$  on the variable  $h$ , conversely the crossing with the section  $\rho$ , the set  $\mathcal{D}_k$  will not be localized, since  $\alpha, \beta$  and  $\omega$  are independent.

Therefore, one must define an event that captures the dynamics of the synchronized time scale. In the pictorial example of Fig. 6 any other piece of section that is a linear combination of  $\mu$  and  $\rho$  provides typical events.

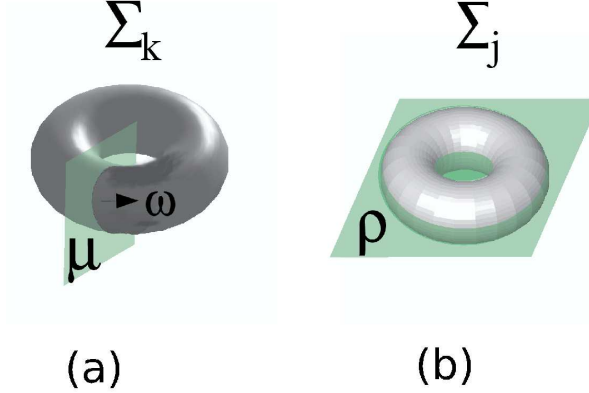


FIG. 6: (Color online) Illustration of two possible sections on the torus  $T^2$ . In (a) the section  $\mu$  takes into account only the dynamics of  $\omega$ , the synchronized scale. In (b) on the other hand, the dynamics of the synchronized time scale is ruled out on the section  $\rho$ . Therefore, using this particular section one cannot observe localized sets  $\mathcal{D}$ , since the synchronized time-scale is not taken into account.

### B. Spiking/Bursting Dynamics

An interesting situation is when the time scales present a relationship, which is the case for spiking/bursting oscillators. Consider two spiking/bursting neurons  $\mathcal{N}_j$  and  $\mathcal{N}_k$ . They have distinct time-scales, the bursting scale, with low frequencies, and the spiking scale, with high frequencies.

The spiking scale consists of the action potentials [28] which occur due to the exchange of ions like  $K^+$  of the external media with the neuron. On the other hand, the neuron may also exchange slow current like  $Ca^{+2}$  which inhibits the occurrence of spikes generating the bursts. An event defined by the occurrence of a burst defines simultaneously the beginning and the ending of a spike train. Therefore, even though spikes and bursts may have independent frequencies, the burst occurrence is also determined by the occurrence of the first and last spike within the burst.

It has been reported that it is possible to have PS in the bursting scale while the spiking scale is not synchronized [6]. Therefore, in order to analyze the existence of synchronization between the neurons, by means of standard techniques, the spiking and bursting scales must be separately analyzed. Our method detects PS independently on the time-scale that the event is defined; if one time-scale is synchronous one finds localized  $\mathcal{D}$  sets. In order to

illustrate this result we may take the following example. Assume that the bursting scales are strongly synchronized. This means that if neuron  $\mathcal{N}_j$  ends the  $i$ th burst at a time  $t_j^i$ , the neuron  $\mathcal{N}_k$  ends the  $i$ th burst at a time  $t_k^i = t_j^i + \xi^i$ , where  $\xi^i \approx O(\eta) \ll O(1)$ . Next, consider that within any burst in neuron  $\mathcal{N}_j$  there are always two spikes equidistant in time. Let us denote  $\tau_j^n$  the time at which the  $n$ th spike occurs in  $\mathcal{N}_j$ . In neuron  $\mathcal{N}_k$  there are two spikes within a burst and with a probability  $p_k$  a third spike may occur [ Fig. 7(a)]. Under this construction, it is clear that the spiking scales are not synchronized.

We can verify this by applying the same approach as in Refs. [6, 12]. We define a threshold for the burst occurrence, the dot gray line in Fig. 7(a). Then for every burst we assume that the phase  $\phi$  is increased by  $2\pi$  and between two bursts the phase increases linearly. So, the phase for the neuron  $\mathcal{N}_k$  can be written as:

$$\phi_k(t) = 2\pi \times \left( i + \frac{t - t_k^i}{t_k^{i+1} - t_k^i} \right). \quad (14)$$

A similar equation can be written for  $\mathcal{N}_j$ . Note only that at a time  $t$ , the neuron  $\mathcal{N}_j$  may present  $m$  bursts. So, the phase difference  $|\Delta\phi| = |\phi_k(t) - \phi_j(t)|$  is equal to  $|2\pi \times \left( i + \frac{t - t_k^i}{t_k^{i+1} - t_k^i} \right) - 2\pi \times \left( m + \frac{t - t_j^m}{t_j^{m+1} - t_j^m} \right)|$ . Now bringing the fact that  $|t_k^i - t_j^i| < O(\eta)$ , we have

$$|\Delta\phi| < 4\pi. \quad (15)$$

Therefore, the phase difference is bounded. On the spiking scale the situation is different; there is no synchronization. Doing the same procedure, we introduce a phase  $\psi$  that is increased by  $2\pi$  between two successive spikes. Thus, the phase for the neuron  $\mathcal{N}_k$  can be written as:

$$\psi_k(t) = 2\pi \times \left( n + \frac{t - \tau_k^n}{\tau_k^{n+1} - \tau_k^n} \right). \quad (16)$$

A naive computation in the limit  $t \rightarrow \infty$  shows that  $|\Delta\psi| \approx p_k n$ . Hence, there is, of course, no synchronization on the spiking scale.

Next, we construct the set  $\mathcal{D}_j$  observing the neuron  $\mathcal{N}_j$  every time that an event happens in the neuron  $\mathcal{N}_k$ . First, we fix the event to be the ending of a burst, see Fig. 7(a). As we observe  $\mathcal{N}_j$  at  $t_k^i$  all the points of  $\mathcal{D}_j$  will be close to the end of the burst. So, the set  $\mathcal{D}_j$  does not spread over the attractor, see the gray points in Fig. 7(b). However, the set  $\mathcal{D}_j$  is also localized even if we set the event to be the occurrence of a spike. Since the spikes always occur within a burst, even though the spikes themselves are not synchronized, the

trajectory related to the hyperpolarization period will not be visited, and therefore, the set  $\mathcal{D}_j$  will be localized, see the black balls in Fig. 7(b).

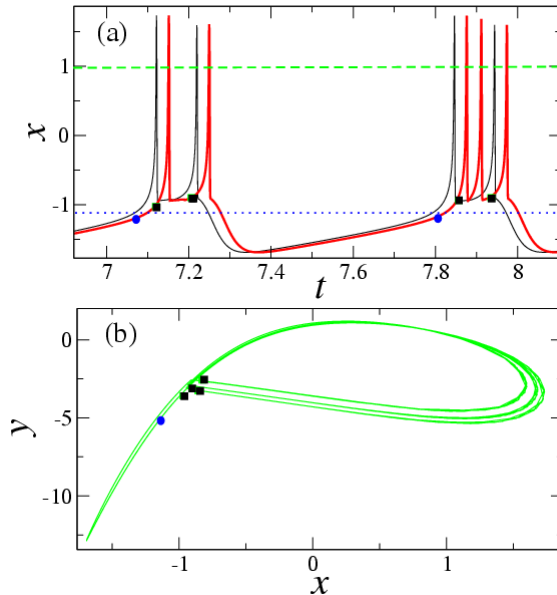


FIG. 7: (Color online) In (a) we present the time series of the membrane potential of two neurons  $\mathcal{N}_k$  and  $\mathcal{N}_j$  in light gray and black respectively. We show the threshold, in dashed line, for the burst occurrence, and in light gray dots, for the spike occurrence. While the bursting scale is synchronized the spiking scale is not. However, both scales can be used to construct the sets  $\mathcal{D}$  and they will be localized due to the synchronization in the bursting scale. In (b), we show the set  $\mathcal{D}_k$  constructed using the spiking scale (black balls) and the set  $\mathcal{D}_k$  constructed using the bursting scale (black squares). As one can see both are localized.

## VI. NEURONAL DYNAMICS

Next, we study the appearance of PS between two spiking/bursting neurons of the Hindmarsh-Rose (HR) type. In such an oscillator the introduction of a phase is rather difficult, since the neurons are non-coherent. We couple the neurons via inhibitory synapses, which introduces non-coherence in both time-scales. This happens because when one neuron spikes it inhibits the other neuron, which hyperpolarizes, but the neuron that has been inhibited still tries to spike. This competition generates even more non-coherence in both time-scales. Therefore, we consider this model as a proper example to illustrate our results.

In the 4-dimensional HR model [5, 29] neurons are described by a set of four coupled differential equations:

$$\begin{aligned}
\dot{x}_k &= ay_k + bx_k^2 - cx_k^3 - dz_k + I_k + g_{syn} \mathbf{C} \mathbf{I}_{syn}(\mathbf{x}) \\
\dot{y}_k &= e - y_k + fx_k^2 - gw_k, \\
\dot{z}_k &= \mu(-z_k + R(x_k + H)), \\
\dot{w}_k &= \nu(-kw_k + r(y_k + l)),
\end{aligned} \tag{17}$$

where  $x_k$  represents the membrane potential of the neuron  $\mathcal{N}_k$ ,  $y_k$  is associated with fast currents exchange and  $(z_k, w_k)$  with slow currents dynamics,  $\mathbf{I}_{syn}(\mathbf{x}) = (I_{syn}(x_1), I_{syn}(x_2), \dots, I_{syn}(x_N))$  is the synaptic input vector and  $I_{syn}(x_j)$  is the synaptic current that neurons  $\mathcal{N}_j$  (post-synaptic) injects in  $\mathcal{N}_k$  (pre-synaptic), and  $\mathbf{C} = \{c_{kj}\}$  is the  $N \times N$  connectivity matrix where  $c_{kj} = 1$  if neuron  $\mathcal{N}_j$  is connected to neuron  $\mathcal{N}_k$ , and  $c_{kj} = 0$ , otherwise, with  $j \neq k$ . This model has been shown to be realistic, since it reproduces the membrane potential of biological neurons [30], and it is able to replace a biological neuron in a damaged biological network, restoring its natural functional activity [31]. It also reproduces a series of collective behaviors observed in a living neural network [5]. The parameters of the model are the same as in Ref. [5], but the intrinsical current  $I_k$ . We change  $I_k$  in order to obtain a spiking/bursting behavior and we use it as a mismatch parameter. First, we consider two neurons  $\mathcal{N}_j$  and  $\mathcal{N}_k$ . In the following, we consider the parameters  $I_k = 3.1200$ ,  $I_j = 3.1205$  and  $g_{syn} = 0.85$ .

The chemical synapses [32] are modeled by:

$$\begin{aligned}
I_{syn}(x_j) &= S(t) (x_{rev} - x_j), \\
[1 - S_\infty(x_i)] \tau \dot{S}(t) &= S_\infty(x_i) - S(t),
\end{aligned} \tag{18}$$

where  $x_j$  is the post-synaptic neuron,  $x_{rev}$  is the reversal potential for the synapse, and  $\tau$  is the time-scale governing the receptor binding.  $S_\infty$  is given by:

$$S_\infty(x_i) = \begin{cases} \tanh\left(\frac{x_i - x_{th}}{x_{slope}}\right), & \text{if } x_i > x_{th} \\ 0 & \text{otherwise} \end{cases} \tag{19}$$

The synapse parameters are  $x_{th} = -0.80$ ,  $x_{slope} = 1.00$ ,  $x_{rev} = -1.58$ . They are chosen in such a way to obtain an inhibitory effect in the chemical synapse.



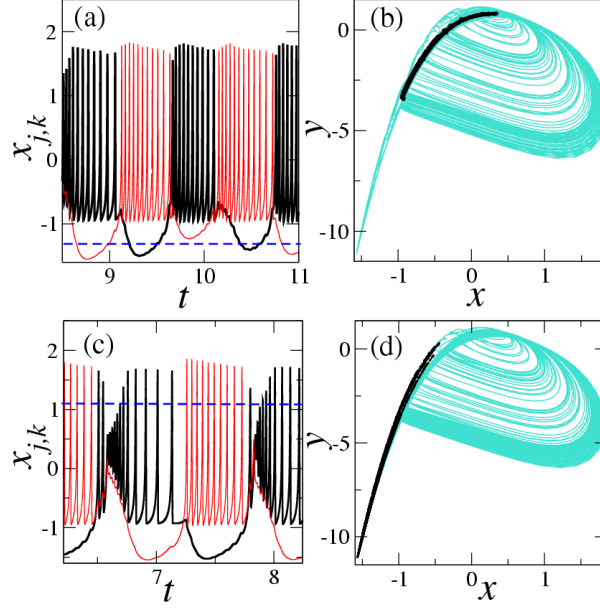


FIG. 8: (Color Online) PS between two HR neurons coupled via inhibitory synapses. We analyze the effect of different threshold levels on the detection of PS. We depicted the attractor projection  $(x, y)$  in gray, and the set  $\mathcal{D}_k$  in black, for Figs. (b) and (d). In (a) the time series of the membrane potentials (full lines) and the threshold  $x_b = -1.3$  (dashed line) are depicted. In (b) the set  $\mathcal{D}_k$ , construct by means of the threshold  $x_b$ , is localized; showing the presence of PS. The time series of the membrane potentials (full lines) and the threshold  $x_s = 1.1$  (dashed line) are depicted in (c). The spikes are not in PS. With our method, even for this threshold one can obtain a localized set. In (d), the set  $\mathcal{D}_k$  construct by using the threshold  $x_s = 1.1$  is localized.

To construct the sets  $\mathcal{D}$ , we define the event occurrence. We shall analyze two situations: when the event is defined in the bursting scale, and when the event is defined in the spiking scale. Firstly, we define the  $i$ th event to be the  $i$ th crossing of the membrane potential of the neuron  $\mathcal{N}_{j,k}$  with the threshold  $x_b = -1.3$  in an upwards direction. We denote the time events by  $t_{j,k}^i$ . Note that this threshold assigns to the times  $t_{j,k}^i$  the beginning of the  $i$ th burst of  $\mathcal{N}_{j,k}$ . Fig. 8(a) shows the time series of the membrane potential of the neurons  $\mathcal{N}_{j,k}$ . The threshold  $x_b = -1.3$  is depicted with the dashed line, and it is chosen in such a way that it does not define a proper Poincaré section, which means that not all the bursts cross it, see Fig 8(a). Actually many bursts are missed. Thus, the approach to extract the phase considering the increasing of  $2\pi$  between two bursts, misleads the statement of PS. That is so, because in this approach the phase is threshold dependent. Therefore, by using Eq.

(14), we get that PS does not exist, which is crucially wrong (note that, with the increasing of the threshold value PS would appear). However, our approach, which is not threshold dependent, overcomes these difficulties. Indeed, localized sets exist even for this threshold [Fig 8(b)].

Conversely, if we increase the threshold level in such a way that it takes into account the spike occurrence, e.g. a threshold at  $x_s = 1.1$ , the dashed line in Fig. 8(c), the former approach, as in Eq. (16), completely fails to state PS, due to the fact that the spikes are not in PS. Furthermore, the spikes are highly non-coherent. The competition between the two neurons generates a damping in the spikes in the beginning of the burst, followed by an increasing and then decreasing in the spike frequency [Fig. 8(c)]. Again, since the threshold  $x_s = 1.1$  defines a typical event, the observation of  $\mathcal{N}_{j,k}$  at times  $(t_{k,j}^i)_{i \in \mathbb{N}}$  provides localized sets  $\mathcal{D}$  [ Fig. 8(d)].

## VII. EXCITATORY NEURAL NETWORKS

The ideas introduced herein are also useful to analyze the onset of synchronization in networks. We consider a network of 16 non-identical HR neurons, regarded as  $\mathcal{N}_i$  where  $i \in [1, \dots, 16]$ , connected via excitatory chemical synapses. The mismatch parameter is the intrinsic current  $I_i$ . Since the meaningful parameter is  $I_i = 3.12$ , for which the HR neuron best mimics biological neurons, we introduce mismatches around this value for all the neurons within the network. Thus, given a random number  $\eta_i$  uniformly distributed within the interval  $[-0.05, 0.05]$ , we set  $I_i = 3.12 + \eta_i$ . The excitatory synapses are modeled by Eqs. (18) and (19). To obtain the excitatory effect we change the value of  $x_{rev}$ . If  $x_{rev} \geq x_i(t)$ , the pre-synaptic neuron always injects a positive current in the post-synaptic one. Since the maximum spike amplitude is around 1.9, we set  $x_{rev} = 2.0$ .

Our network is a homogeneous random network, i.e. all neurons receive the same number  $k$  of connections, namely  $k = 4$ , see Fig. 9(a). We constrain  $g_{syn}$  [see Eq. (17)] to be equal to all neurons. We identify the amount of phase synchronous neurons by analyzing whether the sets  $\mathcal{D}_i$  are localized.

The onset of PS in the whole network takes place at  $g_{syn}^* \approx 0.47$ ; so all neurons become phase synchronized. As the synapse strength crosses another threshold,  $\tilde{g}_{syn} \approx 0.525$ , the neurons undergo a transition to the rest state no longer presenting an oscillatory behavior.

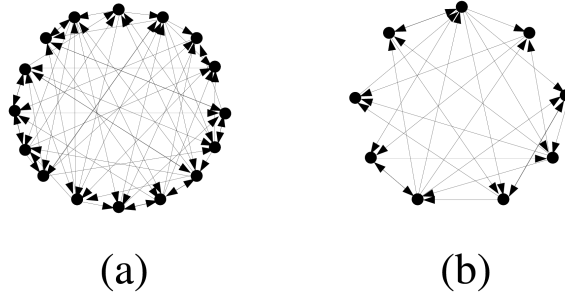


FIG. 9: Networks generated randomly. In (a)  $n=16$  and  $k=4$ , while in (b)  $n=9$  and  $k=3$ .

Clusters of PS appear for  $g_{syn} \ll g_{syn}^*$ . In fact, right at  $g_{syn} \approx 0.04$ , some PS clusters appear [Fig. 10(a)]. Again, the clusters are identified by analyzing the localized sets. These clusters seem to be robust under small perturbations.

Clusters of PS inside the network may offer a suitable environment for information exchanging. Each one can be regarded as a channel of communication, since they possess different frequencies, each channel of communication operates in different bandwidths. To see the bandwidths in the network, we analyze the variance in the average bursting time of the neurons. Since only the burst scale is synchronized, we are just interested in the average bursting time, which can be straightforwardly estimated with a fast Fourier transformation FFT [33]. So, given the neuron  $\mathcal{N}_j$ , we label its bursting average time by  $\langle T_j \rangle$ . Then, we compute the variance of the average time on the ensemble of neurons. For this, we first introduce the average time of the whole network, which is given by:

$$\zeta = \frac{1}{n} \sum_{j=1}^n \langle T_j \rangle. \quad (20)$$

Thus, the variance of the average time on the ensemble of neurons is readily written as:

$$\sigma = \frac{1}{n} \sum_{j=1}^n (\langle T_j \rangle - \zeta)^2. \quad (21)$$

So,  $\sigma$  indicates how diverse are the bandwidths. As one can see in Fig 10(b), when the first clusters appear for  $g_{syn} \approx 0.04$ , we have  $\sigma \approx 0$  indicating that the whole network is working almost with the same frequency. A further increasing of  $g_{syn}$  causes the destruction of these clusters and an increasing of  $\sigma$ . However, even in the regimes of high  $\sigma$  with  $g_{syn} \in [0.27, 0.34]$ , there is the formation of clusters.

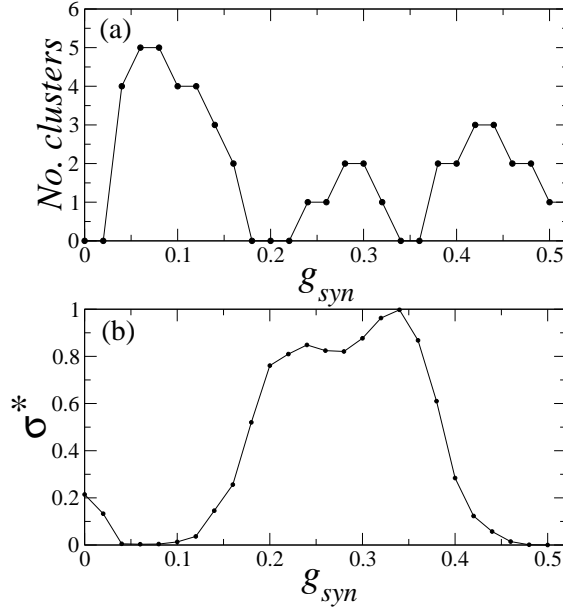


FIG. 10: The appearance of PS clusters within the network. In (a) we show the number of clusters as a function of the synaptic strength. In (b) we plot the normalized  $\sigma^*$ , where  $\sigma^* = \sigma/112.8$ . Note that when the clusters are formed  $\sigma$  becomes small, but bounded away from zero, which means that the neurons within the network undergo a transition where they have almost the same frequency.

This scenario of cluster formation is neither restricted to this HR model nor to the synapse model. It can also be found in square-wave and parabolic bursters, and it is in general achieved quite before the onset of complete synchronization. For example, we use a more simplified HR model given by:  $\dot{x}_j = ax_j^2 - x_j^3 - y_j - z_j - g_{syn}(x_j - x_s)\mathbf{C}\mathbf{I}_{syn}(\mathbf{x})$ ,  $\dot{y} = (a + \alpha)x^2 - y$ ,  $\dot{z} = \mu(bx + c - z)$ , with the parameters:  $a = 2.8$ ,  $\alpha = 1.6$ ,  $c = 5$ ,  $b = 9$ ,  $\mu = 0.001$ ;  $\mathbf{C}$  being the connectivity matrix and  $\mathbf{I}_{syn}(\mathbf{x}) = (I_{syn}(x_1), \dots, I_{syn}(x_N))$  a fast threshold modulation as synaptic input given by

$$I_{syn}(x_j) = 1/[1 + \exp\{-\beta(x_j - \Theta)\}], \quad (22)$$

with  $\beta = 10$  and  $\Theta = -0.25$ . As before,  $g_{syn}$  is the synaptic strength and the reversal potential  $x_s > x_j(t)$  in order to have an excitatory synapse. For a homogeneous random network of 9 identical HR neurons, with  $k = 3$  [ Fig. 9(b)], the theory developed in Ref. [34] predicts the onset of complete synchronization at  $\bar{g}_{syn} \approx 0.425$ , while we found that PS in the whole network is already achieved at  $g_{syn}^* \approx 0.36$ . Clusters of PS, however, appear

for a much smaller value of the coupling strength, actually at  $g_{syn} \approx 0.03$ . Next, we apply the same procedure as before and we compute the variance of the average bursting time on the ensemble of neurons within the network. The result  $\sigma \times g_{syn}$  is depicted in Fig. 11, the inset numbers indicate the amount of clusters.

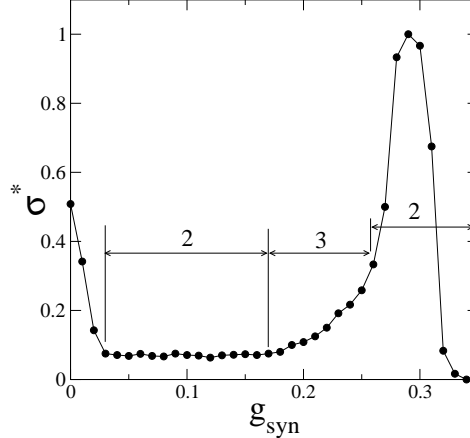


FIG. 11: The average bursting time on the ensemble of neurons. We plot the normalized  $\sigma^*$ , where  $\sigma^* = \sigma/12$ . The inset numbers show the amount of clusters for a given parameter  $g_{syn}$

As we have pointed out, such clusters are rather suitable for communication exchanging mainly for two reasons: *(i)* They have different frequencies, therefore, each cluster may be used to transmit information in a particular bandwidth, which may provide a multiplexing processing of information. *(ii)* The clusters of phase synchronous neurons provide a multichannel communication, that is, one can integrate a large number of neurons (chaotic oscillators) into a single communication system, and information can arrive simultaneously at different places of the network. This scenario may have technological applications, e.g. in digital communication [37, 38], and it may also guide us towards a better understanding of information processing in real neural networks [15, 16, 39].

### VIII. DETECTION OF PS FOR HIGHER DIMENSIONAL SYSTEM

It is easy to say whether the set  $\mathcal{D}$  is localized in a two dimensional plane; this could be done for example by visual inspection. In multi-dimensional system it might not be

obvious whether the set  $\mathcal{D}$  is localized. This is mainly due to the fact that in a projection of a higher dimensional system onto a low dimensional space, the set  $\mathcal{D}$  might fulfill the projected attractor. Therefore, the analysis of the localization might have to be realized in the full attractor of the subsystem.

The analysis is also relatively easy if we bring about a property of the conditional observation. Whenever there is PS, the conditional observation, given by  $\mathbf{F}_j^{t_k^i}(\mathbf{x}_j^0)$ , is not topologically transitive [35] in the attractor of  $\Sigma_j$ , i.e.  $\mathcal{D}$  is localized. The conditional observations  $\mathbf{F}_j^{t_k^i}(\mathbf{x}_j^0)$  are topologically transitive in the attractor  $\mathcal{A}_j$  of  $\Sigma_j$  [36] if for any two open sets  $\mathcal{B}, \mathcal{C} \subset \mathcal{A}$ ,

$$\exists t_k^{n_i} / \mathbf{F}_j^{t_k^{n_i}}(\mathcal{B}) \cap \mathcal{C} \neq \emptyset. \quad (23)$$

To check whether  $\mathcal{D}_j$  is localized, we do the following. If there is PS, for  $\mathbf{y}_j \in \mathcal{D}_j$  it exists infinitely many  $\mathbf{x}_j \in \mathcal{A}_j$  such that

$$\mathbf{y}_j \cap B_\ell(\mathbf{x}_j) = \emptyset, \quad (24)$$

where  $B_\ell(\mathbf{x}_j)$  is an open ball of radius  $\ell$  centered at the point  $\mathbf{x}_j$ , and  $\ell$  is small. We may vary  $\mathbf{y}_j$  and  $\mathbf{x}_j$  to analyze whether it is possible to fulfill Eq. (24). Whenever this is possible, it means that the set  $\mathcal{D}_j$  does not spread over the attractor of  $\Sigma_j$ , and therefore, there is PS.

For analysis of PS basing on experimental data [11, 18, 20] where the relevant dynamical variables can be measured, so that the phase space is recovered, our approach can be used straightforwardly. If one just has access to a bivariate time series, one first has to reconstruct the attractors, and then proceed the PS detection by our approach

## IX. INFORMATION TRANSMISSION

In this section, we analyze the relationship between the sets  $\mathcal{D}$  and the capacity of information transmission between chaotic oscillators. In order to proceed such an analysis, we may assume that the oscillators are identical or nearly identical. Such that the synchronized trajectories are not far from the synchronization manifold, i.e. the subspace where  $\mathbf{x}_j = \mathbf{x}_k$  [2, 3]. Next, for a sake of simplicity we consider only oscillators whose trajectory possess a

proper rotation and are coherent [22, 38], e.g. the standard Rössler oscillator. However, the ideas herein can be extended to other oscillators as well.

The amount of information that two systems  $\Sigma_j$  and  $\Sigma_k$  can exchange is given by the mutual information  $I(\Sigma_j, \Sigma_k)$  [40]:

$$I(\Sigma_j, \Sigma_k) = H(\Sigma_j) - H(\Sigma_j|\Sigma_k), \quad (25)$$

where  $H(\Sigma_j)$  is the entropy of the oscillator  $\Sigma_j$  and  $H(\Sigma_j|\Sigma_k)$  is the conditional entropy between  $\Sigma_j$  and  $\Sigma_k$ , which measures the ambiguity of the received signal, roughly speaking the errors in the transmission.

As pointed out in Ref. [14] the mutual information can be also estimated through the conditional exponents associated to the synchronization manifold. The mutual information is given by:

$$I(\Sigma_j, \Sigma_k) = \sum \lambda_{\parallel}^+ - \sum \lambda_{\perp}^+ \quad (26)$$

where  $\lambda_{\parallel}^+$  are the positive conditional Lyapunov exponents associated to the synchronization manifold, the information produced by the synchronous trajectories, and  $\lambda_{\perp}^+$  are the positive conditional Lyapunov exponents transversal to the synchronization manifold, related with the errors in the information transmission. In PS  $\lambda_{\perp}^+$  can be small, which means that one can exchange information with a low probability of errors. So, PS creates a channel for reliable information exchanging [14]. In general, we expect  $\sum \lambda_{\parallel}^+ \leq \sum \lambda^+$ , where  $\lambda^+$  are the positive Lyapunov exponents. Thus  $I(\Sigma_j, \Sigma_k) \leq \sum \lambda^+ - \sum \lambda_{\perp}^+$ . In order to estimate an upper bound for  $I(\Sigma_j, \Sigma_k)$ , we need to estimate  $\lambda_{\perp}^+$ , what can be done directly from the localized sets.

The conditional transversal exponent can be estimated from the localized sets by a simple geometric analysis. At the time  $t_j^i$  the oscillator  $\Sigma_j$  reaches the Poincaré plane at  $\mathbf{x}_j^*$  while the oscillator  $\Sigma_k$  is at  $\mathbf{x}_k^i = \mathbf{x}_k(t_j^i)$ . The initial distance between the trajectories is  $\Delta \mathbf{x}_{jk} = \mathbf{x}_j^* - \mathbf{x}_k^i$ . This distance evolves until the time  $t_k^i$  when the oscillator  $\Sigma_k$  reaches the Poincaré plane at  $\mathbf{x}_k^*$ , while the trajectory of  $\Sigma_j$  is at  $\mathbf{x}_j^i = \mathbf{x}_j(t_k^i)$ . The new distance is  $\Delta \tilde{\mathbf{x}}_{jk}(t_k^i - t_j^i) = \mathbf{x}_k^* - \mathbf{x}_j(t_k^i)$ . Therefore, we have:

$$\Delta \tilde{\mathbf{x}}_{jk} = \Delta \mathbf{x}_{jk} e^{\lambda_{\perp}^+ |t_k^i - t_j^i|} \quad (27)$$

So, the local transversal exponent is given by:

$$\lambda_{\perp}^{+} = \lim_{N \rightarrow \infty} \frac{1}{N} \sum_{i=1}^N \frac{1}{|t_j^i - t_k^i|} \ell n \left| \frac{\mathbf{x}_j^{*} - \mathbf{x}_k^i}{\mathbf{x}_k^{*} - \mathbf{x}_j^i} \right|, \quad (28)$$

where we use the convention  $0 \times \log 0 = 0$ . Of course, we only estimate the conditional exponent close to the Poincaré plane. Hence, if we change the Poincaré plane the conditional exponent may also change, i.e. there are some events that carry more information than others.

### A. Example with Rössler Oscillators

We illustrate this approach for two coupled Rössler oscillators. We set the parameters to  $a = 0.15$ ,  $b = 0.2$ ,  $c = 10$ ,  $\alpha_j = 1$ , and  $\Delta\alpha_k = 0.0002$ . As shown in Ref. [14] at  $\epsilon \approx 0.05$ , the two oscillator undergo a transition to PS. In particular, for  $\epsilon = 0.06$  we have  $\sum \lambda_{\perp}^{+} \approx 0.06$ . We estimate  $\sum \lambda_{\perp}^{+}$  at this situation by means of Eq. (28). We set the Poincaré section at  $y_{j,k} = 0$ , and compute  $\lambda_{\perp}$  for 65,000 cycles, i.e. 65,000 crossing of the trajectory with  $y = 0$  and  $\dot{y} < 0$ . We get  $\lambda_{\perp} \approx 0.048$ . Note that we are not computing  $\sum \lambda_{\perp}^{+}$ , but rather, the maximum  $\lambda_{\perp}^{+}$ , namely  $\tilde{\lambda}_{\perp}^{+}$ . Therefore, it is natural to expect  $\lambda_{\perp}^{+}$  to be smaller than  $\sum \lambda_{\perp}^{+}$ . However, the upper bound to the information exchange can be estimated by  $I(S, R) \leq \sum \lambda^{+} - \tilde{\lambda}_{\perp}^{+}$ , that is, the maximum amount of information that can flow through the coupled oscillators if we encode the trajectory using the Poincaré plane  $y = 0$  [37]. Furthermore, it seems that when the level of synchronization is large, the estimation of  $\tilde{\lambda}_{\perp}^{+}$ , by means of Eq. (28), might become problematic, due to strong fluctuations in  $|t_j^i - t_k^i|^{-1} \ell n[|(\mathbf{x}_j^{*} - \mathbf{x}_k^i)/(\mathbf{x}_k^{*} - \mathbf{x}_j^i)|]$ .

## X. CONCLUSIONS

We have proposed an extension of the stroboscopic map, as a general way to detect PS in coupled oscillators. The idea consists in constraining the observation of the trajectory of an oscillator at these times in which typical events occur in the other oscillator. This approach provides an efficient and easy way of detecting PS, without having to explicitly calculate the phase. We have shown that if PS is present, the maps of the attractor appear as a localized set in the phase-space. This has been illustrated in coherent oscillators, the



coupled Rösslers, as well as in non-coherent oscillators, spiking/bursting neurons of HR type coupled with chemical synapses. As we have shown in neural networks, the appearance of clusters of PS is rather common, which may be relevant for communication mainly due to two aspects: (i) The clusters provide multiplexing information processing, namely each cluster may be used to transmit information within a bandwidth. (ii) They provide a multichannel communication, that is, a large number of neurons is integrated into a single communication system. Moreover, we have analyzed the relation between the information exchanging and the localized sets. We have roughly estimated the errors in the information transmission from the localized sets.

**Acknowledgment** We would like to thank M. Thiel, M. Romano, C. Zhou, and L. Pecora for useful discussions. This work was financially supported by the Helmholtz Center for Mind and Brain Dynamics, EU COST B27 and DFG SPP 1114.

## APPENDIX A: PROOF OF THEOREM 1

In this appendix we prove the theorem 1. It is instructive to give a sketch of the proof, in order to have a better understanding of the result. We split the demonstration into the following four steps: (i) We show that the increasing of  $2\pi$  in the phase  $\phi_{j,k}$  defines a smooth section  $\Gamma_{j,k}$  on  $\Sigma_{j,k}$ , which does not intersect itself. (ii) We show that observing the oscillator  $\Sigma_j$  whenever oscillators  $\Sigma_k$  crosses  $\Gamma_k$  gives place to a localized set  $\mathcal{D}_j$ . (iii) Further, we show that the observation of  $\Sigma_j$  whenever  $\Sigma_k$  crosses a piece  $P_{\Gamma_k}$  of the section  $\Gamma_k$  also gives place to a localized set. (iv) Using these results we show that, actually, the localized sets can be constructed using any typical event. To show this, we only note that given a typical event with positive measure, we can choose  $P_{\Gamma_k}$  to be close to the event occurrence, implying that shortly before or shortly after of every event occurrence, a crossing of the trajectory with  $P_{\Gamma_k}$  will happen. Thus, if we observe  $\Sigma_j$  whenever the event occurs in  $\Sigma_k$  we will have a set that is close to  $\mathcal{D}_j$ , and therefore, localized. Next, we formalize the heuristic ideas. Let us introduce  $i = j, k$ .

**Proposition 2** *The increasing of  $2\pi$  in  $\phi_i(t)$  generates a smooth section  $\Gamma_i$  in the attractor of  $\Sigma_i$ , which does not intersect itself.*

*Proof:* Firstly, let us introduce the times  $(\tau_i^m)$  such that  $\phi_i(\tau_i^m) = m \times 2\pi$ . Then, let  $\Gamma_i$  be the set of points such that given the initial point  $\mathbf{x}_i^\ell$  we have the section:

$$\Gamma_i = \{\cup_{m \in \mathbb{N}} \mathbf{x}_i^m \mid \mathbf{x}_i^m = \mathbf{F}_i^{\tau_i^m}(\mathbf{x}_i^\ell)\} \quad (\text{A1})$$

Thus, we construct a section  $\Gamma_i$ .  $\Gamma_i$  is smooth since both  $\phi_i$  and  $\mathbf{F}_i^t$  are smooth. Indeed, given two points  $\mathbf{x}_i^0, \mathbf{x}_i^1 \in \Gamma_i$ , with  $d(\mathbf{x}_i^0, \mathbf{x}_i^1) < \epsilon$ , there is a  $r \geq 1$  such that  $\mathbf{F}_i^{\tau_i^r}(\mathbf{x}_i^0), \mathbf{F}_i^{\tau_i^r}(\mathbf{x}_i^1) \in \Gamma_i$ , and

$$d(\mathbf{F}_i^{\tau_i^r}(\mathbf{x}_i^0), \mathbf{F}_i^{\tau_i^r}(\mathbf{x}_i^1)) < \delta. \quad (\text{A2})$$

Furthermore, we can construct a continuous section  $\Gamma_i$ , by conveniently choosing points  $\mathbf{x}_i^\ell$ . The fact that  $\Gamma_i$  does not intersect itself comes from the uniqueness of  $\mathbf{F}_i^t$  [41], and from the fact that the  $\dot{\phi}_i(t) > 0$ , which implies that the phase is an one-to-one function with the trajectory. Note that, obviously, this section depends on the initial conditions.  $\square$

**Lemma 1** *The observation of the oscillators  $\Sigma_j$  whenever the trajectory of  $\Sigma_k$  crosses the section  $\Gamma_k$  gives place to a localized set  $\mathcal{D}_j$  if, and only if, there is PS.*

*Proof:* Let  $\Pi_j$  be the Poincaré map associated to the section  $\Gamma_j$ , such that given a point  $\mathbf{x}_j^n \in \Gamma_j$ , so  $\mathbf{x}_j^{n+1} = \Pi_j(\mathbf{x}_j^n) = F_j^{\Delta\tau_j^{n+1}}(\mathbf{x}_j^n)$ , where  $\Delta\tau_j^n = \tau_j^n - \tau_j^{n-1}$ . From now on, we use a rescaled time  $t' = t/\langle T_j \rangle$ , with  $\langle T_j \rangle = \lim_{i \rightarrow \infty} \tau_j^i/i$ . For a slight abuse of notation we omit the  $\iota$ . There are numbers  $\kappa_i$  such that  $|\tau_i^i - i\langle T_i \rangle| \leq \kappa_i$ , where, by time reparametrization,  $\kappa_i \ll 1$ . If both oscillators are in PS, then  $\langle T_k \rangle = \langle T_j \rangle$ , and so:

$$|\tau_k^n - \tau_j^n| \leq \tilde{\kappa}, \quad (\text{A3})$$

with  $\tilde{\kappa} \leq \kappa_k + \kappa_j \ll 1$  [42]. Now, we analyze one typical oscillation, using the basic concept of recurrence. Given the following starting points  $\mathbf{x}_k^0 \in \Gamma_k$  and  $\mathbf{x}_j^0 \in \Gamma_j$ , we evolve both until  $\mathbf{x}_j^0$  returns to  $\Gamma_j$ . Let us introduce

$$\Delta\tau^n = \Delta\tau_j^n - \Delta\tau_k^n. \quad (\text{A4})$$

Which gives:

$$\mathbf{F}_j^{\Delta\tau_j^1}(\mathbf{x}_j^0) = \Pi_j(\mathbf{x}_j^0) = \mathbf{x}_j^1 \in \Gamma_j. \quad (\text{A5})$$

Analogously,

$$\begin{aligned}
\mathbf{F}_k^{\Delta\tau_j^1}(\mathbf{x}_k^0) &= \mathbf{F}_k^{\Delta\tau_k^1 + \Delta\tau^1}(\mathbf{x}_k^0) \\
&= \mathbf{F}_k^{\Delta\tau^1} \circ \mathbf{F}_k^{\Delta\tau_k^1}(\mathbf{x}_k^0).
\end{aligned}$$

Bringing the fact that  $\mathbf{F}_k^{\Delta\tau_k^1}(\mathbf{x}_k^0) = \Pi_k(\mathbf{x}_k^0) = \mathbf{x}_k^1$ , we have:

$$\mathbf{F}_k^{\Delta\tau_j^1}(\mathbf{x}_k^0) = \mathbf{F}_k^{\Delta\tau^1}(\mathbf{x}_k^1). \quad (\text{A6})$$

Now, by using the fact that  $|\Delta\tau^i| < \tilde{\kappa}$ , we can write:

$$\mathbf{F}_k^{\Delta\tau^1}(\mathbf{x}_k^1) \approx \mathbf{x}_k^1 + \mathbf{G}(\mathbf{x}_k^1)\tilde{\kappa} + \mathcal{O}(\tilde{\kappa}^2). \quad (\text{A7})$$

So, given a point  $\mathbf{x}_k \in \Gamma_k$  evaluated by the time when the trajectory of  $\Sigma_j$  returns to the section  $\Gamma_j$ , the point  $\mathbf{x}_k$  returns near the section  $\Gamma_k$ , and vice-versa. Therefore, it is localized. For a general case, we have to show that a point, in the section  $\Gamma_k$ , evolved by the flow for an arbitrary number  $N$  of events in the oscillator  $\Sigma_j$ , still remains close to  $\Gamma_k$ , in other words, it is still localized. This is straightforward, since  $|\sum_{i=0}^N \Delta\tau^i| = |\tau_k^N - \tau_j^N| < \tilde{\kappa}$ . So, we demonstrated that the PS regime implies the localization of the set  $\mathcal{D}_k$ .

Now, we show that the localization of the set  $\mathcal{D}_k$  implies PS. Supposing that we have a localized set  $\mathcal{D}_k$ , so, Eq. (A3) is valid, by the above arguments. Therefore, we just have to show that Eq. (A3) implies PS. With effect, we have  $|\phi_j(t) - \phi_k(t)| = |\int_0^t \Omega_j dt - \int_0^t \Omega_k dt|$  which is equal to  $|\int_0^{\tau_j^n} \Omega_j dt - \int_0^{\tau_j^n} \Omega_k dt + \int_{\tau_j^n}^t \Omega_j dt - \int_{\tau_j^n}^t \Omega_k dt|$ . This may be written as  $|\int_0^{\tau_j^n} \Omega_j dt - \int_0^{\tau_k^n} \Omega_k dt - \int_{\tau_j^n}^{\tau_k^n} \Omega_k dt + \int_{\tau_j^n}^t \Omega_j dt - \int_{\tau_j^n}^t \Omega_k dt|$ . Next, noting that  $\phi_i(\tau_i^n) = 2\pi \times n$ , we get:

$$|\phi_j(t) - \phi_k(t)| \leq M|\tau_j^n - \tau_k^n| + 2\Lambda M, \quad (\text{A8})$$

where  $\Lambda = \max|t_i^n - t_i^{n-1}|$ . Therefore, if the time event difference  $|t_j^n - t_k^n|$  is bounded it implies the boundedness in the phase. Thus, we conclude our result.  $\square$

**Proposition 3** *Let  $(\tau_j^{n_i})_{n_i \in \mathbb{N}}$  be the times at which the trajectory  $\Sigma_j$  crosses a piece  $P_{\Gamma_j}$  of  $\Gamma_j$ . If there is PS, then the observation of the trajectory of  $\Sigma_k$  at times  $(\tau_j^{n_i})_{n_i \in \mathbb{N}}$  gives place of a localized set.*

*Proof:* Note that the observation of the trajectory of  $\Sigma_k$  at times  $(\tau_j^{n_i})_{n_i \in \mathbb{N}}$  gives place to a set  $\mathcal{D}_k$ , while the observations at times  $(\tau_j^{n_i})_{n_i \in \mathbb{N}}$  give place to a subset  $\tilde{\mathcal{D}}_k$  of  $\mathcal{D}_k$ . Therefore, whenever  $\mathcal{D}_k$  is localized, it implies the localized of  $\tilde{\mathcal{D}}_k$ .  $\square$

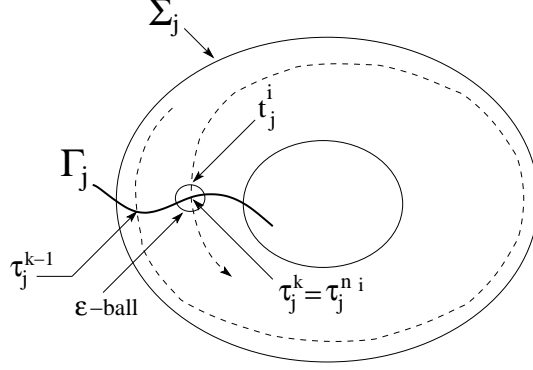


FIG. 12: Illustration of Eq. (A9).

Now, we are ready to prove the *theorem* 1.

*Proof:* Let the event be the entrance in an  $\varepsilon$ -ball, such that the event occurrence produces the time series  $t_j^i$ , in  $\Sigma_j$ . There is, at least, one intersection of this ball with the section  $\Gamma_j$ . Since  $\Gamma_j$  depends on the initial conditions, we can choose an initial condition right at the  $\varepsilon$ -ball event. Next, we choose  $P_{\Gamma_j}$  such that it is completely covered by the  $\varepsilon$ -ball. Since the measure of the  $\varepsilon$ -ball is small,  $\varepsilon \ll 1$ , the time difference between crossings of the trajectory with  $P_{\Gamma_j}$  and the  $\varepsilon$ -ball is small, thus, there is a number  $\eta < 1$  such that:

$$t_j^i - \tau_j^{n_i} \ll O(\eta). \quad (\text{A9})$$

Therefore, if we observe the trajectory of  $\Sigma_k$  at times  $(t_j^i)_{i \in \mathbb{N}}$ , we have a localized set in  $\Sigma_k$ . Thus, we conclude our result: The observation of the trajectory of  $\Sigma_{j,k}$  whenever typical events in  $\Sigma_{k,j}$  occurs generates localized sets  $\mathcal{D}_{j,k}$  if, and only if, there is PS.  $\square$

- 
- [1] H. Fujisika and T. Yamada, Progr. Theoret. Phys. **69**, 32 (1983).
  - [2] L. M. Pecora and T. Carrol, Phys. Rev. Lett. **64**, 821 (1990).
  - [3] L. M. Pecora and T. Carrol, Phys. Rev. Lett. **80**, 2109 (1998).
  - [4] B. Blasius and L. Stone, Nature **406**, 846 (2000); Nature **399**, 354 (1999).
  - [5] R. D. Pinto, P. Varona, A. R. Volkovskii, A. Szucs, H. D. I. Abarbanel, and M. I. Rabinovich, Phys. Rev. E **62**, 2644 (2000).
  - [6] M. V. Ivanchenko, G. V. Osipov, V. D. Shalfeev, and J. Kurths, Phys. Rev. Lett. **93**, 134101 (2004).

- [7] M. Thiel, M.C. Romano, J. Kurths, M. Rolf, and R. Kiegl, *Europhys. Lett.* **75**, 535 (2006).
- [8] P. De Grauwe, H. Wachter, and M. Embrechts *Exchange Rate Theory: Chaotic Models of Foreign Exchange Markets*, (Blackwell, Oxford, 1993).
- [9] I. Leyva, E. Allaria, S. Boccaletti, *et al.* *Phys. Rev. E* **68**, 066209 (2003).
- [10] I. Fischer, Y. Liu, P. Davis, *Phys. Rev. A* **62**, 011801 (2000).
- [11] D. J. DeShazer, R. Breban, E. Ott, R. Roy, *Phys. Rev. Lett.* **87**, 044101 (2001).
- [12] A. Pikovsky, M. Rosenblum, and J. Kurths, *Synchronization: A Universal Concept in Non-linear Sciences*, (Cambridge University Press, 2001); S. Boccaletti, J. Kurths, G. Osipov, D. Valladares, and C. Zhou, *Phys. Rep.* **366**, 1 (2002); J. Kurths, S. Boccaletti, C. Grebogi, *et al.* *Chaos* **13**, 126 (2003).
- [13] M.G. Rosenblum, A.S. Pikovsky and J. Kurths, *Phys. Rev. Lett.* **76**, 1804 (1996); A.S. Pikovsky, M.G. Rosenblum, and J. Kurths, *Physica D.* **76**, 1804 (1997).
- [14] M.S. Baptista and J. Kurths, *Phys. Rev. E* **72**, 045202R (2005).
- [15] F. Mormann, T. Kreuz, R. G. Andrzejak, P. David, K. Lehnertz, and C. E. Elger, *Epilepsy Research* **53**, 173 (2003).
- [16] J. Fell, P. Klaver, C. E. Elger, and G. Fernandez, *Rev. in the Neurosciences* **13**, 299 (2002).
- [17] U. Parlitz, L. Junge, W. Lauterborn, and L. Kocarev, *Phys. Rev. E* **54**, 2115 (1996).
- [18] M. S. Baptista, T. Pereira, J. C. Sartorelli, I. L. Caldas, and E. Rosa, Jr. *Phys. Rev. E* **67**, 056212 (2003).
- [19] I. Z. Kiss and J. L. Hudson, *Phys. Rev. E*, **64**, 046215 (2001).
- [20] C.M. Ticos, E. Rosa, Jr., W.B. Pardo, J.A. Walkenstein, and M. Monti, *Phys. Rev. Lett.* **85**, 2929 (2000).
- [21] D. Maraun and J. Kurths, Epochs of phase coherence between El Nio/ Southern Oscillation and Indian monsoon. *Geophys. Res. Lett.* **32**, L15709 (2005).
- [22] K. Josić and M. Beck, *Chaos* **13**, 247 (2003); K. Josić and D. J. Mar, *Phys. Rev. E* **64**, 056234 (2001).
- [23] C. Schäfer, M.G. Rosenblum, J. Kurths, and H.-H. Abel, *Nature* **392**, 239 (1998).
- [24] M.S. Baptista, T. Pereira, J.C. Sartorelli, I.L. Caldas, and J. Kurths, *Physica D* **212**, 216 (2005).
- [25] R.Q. Quiroga, A. Kraskov, T. Kreuz, P. Grassberger, *Phys. Rev. E* **65**, 041903 (2002).
- [26] We consider  $\text{vol}$  to be the euclidian volume that contains all the points of the set  $\mathcal{D}$ . Thus, if

the set  $\mathcal{D}$  is spread over a sphere of radius  $r$  the volume of the set  $\mathcal{D}$  will be  $\pi r^3$ . The same is valid for the attractor volume.

- [27] Note the the choice of  $H_{jk}$  is somewhat arbitrary. We could also compare the euclidian distance between the points of the attractor and the points of the localized set. This would lead to the approach of Ref. [25].
- [28] E. R. Kandel, J.H. Schwartz, and T.M. Jessel, *Principles of neural science* fourth editon ( Mc Graw Hill, 2000).
- [29] J.L. Hindmarsh, and R.M Rose, Proc. R. Soc. Lond. B. **221**, 87 (1984); J.L. Hindmarsh, and R.M. Rose, Nature **296**, 162 (1982).
- [30] S. W. Johnson, V. Seutin, and R.A. North Science **58**, 665 (1992).
- [31] C. Mulle, A. Madariaga, and M. Deschenes J. Neurosci. **6**, 2134 (1986).
- [32] A. Destexhe, Z.F. Mainen, and T.J. Sejnowski, Neural Comput. **6**, 14 (1994); A.A. Sharp, F.K. Skinner, and E. Narder, J. Neurophysiol. **76**, 867 (1996).
- [33] Sneddon, I. N. *Fourier Transforms*. (Dover, 1995. New York).
- [34] I. Belykh, E. Lange, and M. Hasler, Phys. Rev. Lett **94**, 188101 (2003).
- [35] S. Wiggins, *Introduction to Applied Nonlinear Dynamical Systems and Chaos*, Springer, New York, 1996.
- [36] A chaotic set is always transitive through the flow. So, given a set of initial conditions, its evolution through the flow eventually reaches arbitrary open subsets of the original chaotic attractor. However, the conditional observations might not possesses the transitive property.
- [37] S. Hayes, C. Grebogi, E. Ott, and A. Mark, Phys. Rev. Lett. **73**, 1781 (1994).
- [38] T. Yalçinkaya and Y.C. Lai, Phys. Rev. Lett. **79**, 3885 (1997).
- [39] R. Borisjuk, G Borisjuk, and Y. Kazanovich, Behavior and Brain Sc. **21**, 833 (1998).
- [40] C. E. Shannon, The Bell Syst. Tech. Jour. **27**, 623 (1948).
- [41] L. S. Pontryagin, *Ordinary Differential Equations*, ( Addison-Wesley, 1969).
- [42] We could also show that  $\tilde{\kappa}$  is smaller than 1 by the following argument. Note that the number of crossings  $N_j$  and  $N_k$  of the oscillators  $\Sigma_j$  and  $\Sigma_k$  with the sections  $\Gamma_j$  and  $\Sigma_k$ , respectively, may not be always the same. They can differ by an unity, since the events are not simultaneous. Therefore, we have  $|N_j(t) - N_k(t)| \leq 1$ . However,  $N_i \approx \lim_{t \rightarrow \infty} t / \langle T_i \rangle$ , then, using this into the previous equation and normalizing  $\langle T_j \rangle = 1$ , we have  $|\tau_j^n - \tau_k^n| \leq O(1)$ , for  $n$  large enough.